USING DIRECT AND ADJOINT EIGENFUNCTIONS TO FIND OPTIMAL CONTROL STRATEGIES IN THERMO-ACOUSTICS

Luca Magri* & Matthew P. Juniper

Department of Engineering, University of Cambridge
Trumpington Street, CB21PZ, Cambridge, U.K.
* Corresponding author: lm547@cam.ac.uk

We introduce a linear technique that predicts how the stability of a thermo-acoustic system changes due to the action of a generic passive feedback device and a generic change in the base state. From this, one can calculate the passive device that most stabilizes the system. This method, based on adjoint equations, is applied to two types of thermo-acoustic systems. The first is an electrically heated Rijke tube and the second is a ducted diffusion flame. We find that the most effective passive control device is an adiabatic mesh placed at the downstream end of the Rijke tube. The most receptive regions of the diffusion flame are found and described for open-loop control based on species injection.

1 Introduction

In a thermo-acoustic system, such as a flame in a tube, heat release oscillations couple with acoustic pressure oscillations. If the heat release is sufficiently in phase with the pressure, these oscillations grow, sometimes with catastrophic results [1]. This paper introduces a technique that identifies the most influential changes to the system and determines their effect on stability. It is applied here to two simplified thermo-acoustic systems. When applied to more realistic systems, it will help to identify strategies for passive control of thermo-acoustic oscillations.

The technique is based on adjoint sensitivity analysis, which was proposed for non-reacting incompressible flows by Hill [2]; Giannetti and Luchini [3]; Marquet, Sipp and Jacquin [4]. Adjoint sensitivity analysis of thermo-acoustic systems was proposed by Magri and Juniper [5, 6].

The systems investigated are: a Rijke tube containing an electrically heated hot wire (gauze) [5, 6, 7, 8, 9] and a Rijke tube heated by a diffusion flame [6, 10, 11, 12]. Both heat sources are assumed to be compact so that the acoustic and heat-release models can be decoupled. Both systems have three base-state parameters in common: the position of the heat source, x_f; the heat-release parameter, β; and the acoustic damping, ζ. The electrically heated Rijke tube has one further parameter: a time delay, τ, between velocity and heat-release fluctuations [13]. The ducted diffusion flame has three further parameters, all of which affect the flame shape: the fuel slot width, α; the stoichiometric mixture fraction, Z_{sto}; and the Péclet number, Pe, which is the ratio of mass diffusion timescale / convection timescale.

For the structural sensitivity analysis, shown for the electrically heated Rijke tube, we investigate two passive feedback mechanisms: a second heat source placed in another location along the duct (a second hot wire) and a local smooth variation of the tube cross-sectional area. For the base-state sensitivity analysis, we investigate the influence of the parameters that change the shape of the diffusion flame. Finally, the most receptive regions of a marginally stable diffusion flame are mapped and discussed: these are the regions in which an open-loop species injection is most effective in controlling the frequency and amplitude of the oscillation.

Looking forward, this technique could quickly reveal, for example, the most important components of an acoustic network, the best position for an acoustic damper, the optimal change in the flame shape and could suggest strategies for open-loop control. The usefulness of adjoint techniques applied to thermo-acoustics is that in few calculations we predict accurately how the growth rate and frequency of thermo-acoustic oscillations are affected either by all possible passive control elements in the system (structural sensitivity) or by all possible changes to its base state (base-state sensitivity). This information could be combined with optimization strategies involving other constraints, such as geometrical constraints and a given total heat release rate, to reveal the best control strategies for stabilization of a thermo-acoustic system.

2 Thermo-acoustic models

The two thermo-acoustic systems examined in this paper are horizontal resonant acoustic ducts heated by a compact heat source. The acoustics are modelled in 1-D because the characteristic acoustic length is much greater than the duct width. Acoustic waves take place on top of a *base flow (or mean fluid)*, which undergoes a discontinuity of its uniform properties across the heat source. Only the mean pressure does not undergo a discontinuity in the low Mach number limit. The acoustic momentum and energy equations (called *direct* equations) are, respectively:

$$\rho\frac{\partial u}{\partial t}+\frac{\partial p}{\partial x}=0, \qquad \frac{\partial p}{\partial t}+\frac{\partial u}{\partial x}+\zeta p-\beta\dot{q}\delta_f=0, \tag{1}$$

where u, p and $\dot{q}$ are the non-dimensional velocity, pressure and heat-release rate (scaled by β). The heat source is placed at $x=x_f$ and forces the acoustics as an impulsive term in space modelled with the Dirac delta distribution, $\delta_f\equiv\delta(x-x_f)$. The non-dimensional density is $\rho=\rho_1$ when $x<x_f$ and $\rho=\rho_2$ when $x>x_f$. The positive temperature jump of the base flow, induced by the pointwise heat release, makes the density ratio $\rho_2/\rho_1<1$. The acoustic non-dimensionalization is reported in Magri and Juniper [12]. The acoustic system has three control parameters: ζ, which is the damping; β, which encapsulates all relevant information about heat release, and x_f, which is the position of the heat source. At the ends of the tube, p and $\partial u/\partial x$ are both set to zero. Dissipation and end losses are modelled with the modal damping for each mode j, $\zeta_j=c_1 j^2+c_2\sqrt{j}$, where c_1 and c_2 are the damping constants. This damping model was used in Balasubramanian and Sujith [11] based on correlations developed by Matveev [7].

Two different compact heat-source models are examined in this paper: an electrically heated hot wire (gauze) and an infinite-rate chemistry diffusion flame.

A full description of an electrically heated Rijke tube is given by Juniper [9], based on the model used by Balasubramanian and Sujith [8]. Only the dimensionless form is considered here. The heat-release rate (scaled by β) is modelled as a nonlinear time-delayed function of the velocity [13], which we linearize both in amplitude and time as follows

$$\dot{q}=\frac{\sqrt{3}}{2}\left[u_f(t)-\tau\left(\frac{\partial u(t)}{\partial t}\right)_f\right], \tag{2}$$

where the subscript f means that the variable is evaluated at $x=x_f$. The time delay between the pressure and heat-release oscillations is modelled by the constant coefficient, τ. In the electrically heated Rijke tube, the heat-release parameter β encapsulates all relevant information about the hot wire, base-flow velocity and ambient conditions. Eqn. (2) holds when $|u_f(t-\tau)|\ll 1$ and $\tau\ll 2/K$, where K is the number of Galerkin modes considered in the acoustic discretization.

The ducted diffusion flame is modelled by two different space domains: the 1-D acoustic domain, in which the flame is regarded as a pointwise heat source, and the 2-D flame domain, in which the flame is solved. It is assumed that [10, 11, 12]: the perturbation velocity field of the flame is the acoustic velocity calculated at the flame position, x_f, which is uniform within the 2-D flame domain; the Lewis number is 1; and the combustion occurs along an infinitely thin surface, where the fuel, Y, and the oxidizer, X, are at the stoichiometric ratio (infinite-rate chemistry with one-step reaction). The stoichiometric mass ratio is $s=\nu_x W_x/(\nu_y W_y)$, where W_x and W_y are the molar masses, and ν_x and ν_y are the stoichio-

metric coefficients of the oxidizer and fuel, respectively. The conservative scalar variable Z, also known as Schveb-Zel'dovich variable or mixture fraction, is defined as $Z \equiv (sY - X + X_i)/(sY_i + X_i)$, where the subscript i indicates properties evaluated at the inlet. The stoichiometric surface, where the whole reaction occurs, is the locus of points in which Z assumes the stoichiometric value $Z_{sto} = 1/(1+\phi)$, where $\phi \equiv Y_i/X_i$ is the *equivalence ratio*. The variable Z is split up into two components, $Z = \bar{Z} + \epsilon z$, where $\bar{Z}$ is the analytical steady solution [6, 12], and ϵz is the unsteady field. The non-dimensional combustion domain (ξ, η), where the flame is computed, extends horizontally from 0 to L_c, and vertically from -1 to 1. The parabolic governing equations (PDEs), which the mixture fraction is subject to, are

$$\frac{\partial \bar{Z}}{\partial \xi} - \frac{1}{Pe}\left(\frac{\partial^2 \bar{Z}}{\partial \xi^2} + \frac{\partial^2 \bar{Z}}{\partial \eta^2}\right) = 0, \qquad \frac{\partial z}{\partial t} + \frac{\partial z}{\partial \xi} - \frac{1}{Pe}\left(\frac{\partial^2 z}{\partial \xi^2} + \frac{\partial^2 z}{\partial \eta^2}\right) + u_f \frac{\partial \bar{Z}}{\partial \xi} = -u_f \frac{\partial z}{\partial \xi}, \tag{3}$$

along with the relevant boundary conditions: $\bar{Z}(\xi = 0, \eta) = 1$ when $|\eta| \leq \alpha$, $\bar{Z}(\xi = 0, \eta) = 0$ when $\alpha < |\eta| \leq 1$, $\frac{\partial \bar{Z}}{\partial \eta}(\xi, \eta = \pm 1) = 0$, and $\frac{\partial \bar{Z}}{\partial \xi}(\xi = L_c, \eta) = 0$. The perturbation field z has the same boundary conditions as $\bar{Z}$ except that $z(\xi = 0, \eta) = 0$ when $|\eta| \leq \alpha$. Pe is the Péclet number and α is the non-dimensional fuel slot half width. The non-dimensional combustion parameters are reported in [6]. In linear analysis, the term in the RHS of eqn. (3) is neglected because it is considered to be higher order, i.e. $o(\epsilon)$. The total heat-release rate is given by the integral over the flame space domain (ξ, η) of the total derivative of the sensible enthalpy. The steady heat-release rate depends on whether the flame is closed (overventilated), $Z_{sto} > \alpha$, or open (underventilated), $Z_{sto} < \alpha$. It is $\bar{Q} = 2\alpha$, and $\bar{Q} = 2Z_{sto}(1-\alpha)/(1-Z_{sto})$, respectively. In both cases, the flame tends to assume constant height (infinite length) in the limit $Z_{sto} \to \alpha$. Hence, if the flame is open, the length tends to increase if Z_{sto} increases, vice versa if the flame is closed. For the acoustic energy equation (1) we need to evaluate the fluctuating averaged heat-release rate which is given by:

$$\dot{q} = \int_0^{L_c} \int_{-1}^{1} \theta(Z > Z_{sto}) \left(\frac{-1}{1 - Z_{sto}}\right) \frac{\partial z}{\partial t} \, \mathrm{d}\xi \mathrm{d}\eta + u_f \bar{Q}, \tag{4}$$

where $\theta(Z > Z_{sto})$ is the step function which is 1 in the fuel side $Z > Z_{sto}$, and 0 otherwise.

3 Numerical method

The numerical discretization is performed with the Galerkin method. For the acoustics, we choose as basis functions the natural acoustic modes of the undamped system. The partial differential eqns. (1), which govern the linearized thermo-acoustic system, are discretized into a set of ordinary differential equations by choosing a basis that matches the boundary conditions and the jump condition at $x = x_f$ [14]. The pressure, p, and velocity, u, are expressed as follows [15]

$$p(x,t) = \sum_{j=1}^{K} \begin{cases} -\alpha_j(t) \sin\left(\omega_j \sqrt{\rho_1} x\right), & 0 \leq x < x_f, \\ -\alpha_j(t) \left(\frac{\sin \gamma_j}{\sin \beta_j}\right) \sin\left(\omega_j \sqrt{\rho_2}(1-x)\right), & x_f < x \leq 1, \end{cases} \tag{5}$$

$$u(x,t) = \sum_{j=1}^{K} \begin{cases} \eta_j(t) \frac{1}{\sqrt{\rho_1}} \cos\left(\omega_j \sqrt{\rho_1} x\right), & 0 \leq x < x_f, \\ \eta_j(t) \frac{1}{\sqrt{\rho_1}} \left(\frac{\cos \gamma_j}{\cos \beta_j}\right) \cos\left(\omega_j \sqrt{\rho_2}(1-x)\right), & x_f < x \leq 1, \end{cases} \tag{6}$$

where $\gamma_j \equiv \omega_j \sqrt{\rho_1} x_f$, $\beta_j \equiv \omega_j \sqrt{\rho_2}(1 - x_f)$. The equation which the acoustic frequencies, ω_j, are subject to is $\sin\beta_j \cos\gamma_j + \cos\beta_j \sin\gamma_j \sqrt{\rho_1/\rho_2} = 0$. Note that in the limit of $\rho_1 = \rho_2$, we recover the Galerkin expansion for a base flow with no discontinuity across the flame [8, 9, 11]. Importantly, in this limit the frequencies (as well as the wavenumbers) of the acoustic eigenfunctions are $\omega_j = j\pi$. We use $K = 10$ for the electrically heated Rijke tube and $K = 20$ for the ducted diffusion flame. The unsteady mixture fraction, z, in eqn. (3), is discretized as

$$z(\xi, \eta, t) = \sum_{m=1}^{M} \sum_{n=0}^{N-1} G_{n,m}(t) \cos(n\pi\eta) \sin\left[\left(m - \frac{1}{2}\right) \frac{\pi \xi}{L_c}\right]. \tag{7}$$

We use $M = 35$ and $N = 35$ which is a sufficiently accurate resolution. We checked modal convergence by using $M = 70$ and $N = 70$ and the discrepancy on the dominant eigenvalue was found to be smaller than 0.01%.

4 Applied functional analysis

4.1 Adjoint functions: their definition, calculation and use in stability

The direct and adjoint problems are expressed, respectively, as:

$$\mathrm{A}\frac{\partial \mathbf{q}}{\partial t} - \mathrm{L}\mathbf{q} = \hat{\mathbf{s}}\exp(\sigma_s t), \qquad \mathrm{A}^+\frac{\partial^+ \mathbf{q}^+}{\partial t} - \mathrm{L}^+\mathbf{q}^+ = 0, \tag{8}$$

where $\hat{\mathbf{s}}$ is a forcing term which is set to zero in this section. If eqns. (8) represent the continuous equations, then A, L, A^+, L^+ are operators and $\mathbf{q} = (z, u, p)^T$. In this case, the adjoint operators and equations are analytically derived and then numerically discretized (CA, discretization of Continuous Adjoints). If eqns. (8) represent the numerically discretized systems, then A, L, A^+, L^+ are matrices and $\mathbf{q} = (\mathbf{G}, \eta, \alpha)^T$. In this case, the adjoint matrices and functions are directly derived from the numerically discretized direct system (DA, Discrete Adjoints).

In this paper, the adjoint systems are defined through a bilinear form $\langle \cdot, \cdot \rangle$ which is an inner product[1], such that:

$$\left\langle \mathbf{q}^+, \left(\mathrm{A}\frac{\partial}{\partial t} - \mathrm{L}\right)\mathbf{q} \right\rangle - \left\langle \left(\mathrm{A}^+\frac{\partial^+}{\partial t} - \mathrm{L}^+\right)\mathbf{q}^+, \mathbf{q} \right\rangle \doteq \text{constant}. \tag{9}$$

To find the adjoint operator with the CA approach we have to perform integration by parts of

$$\int_T\int_V \mathbf{q}^{+*}\cdot\left(\mathrm{A}\frac{\partial}{\partial t} - \mathrm{L}\right)\mathbf{q}\,\mathrm{d}V\mathrm{d}t - \int_T\int_V \left(\mathrm{A}^+\frac{\partial^+}{\partial t} - \mathrm{L}^+\right)^* \mathbf{q}^{+*}\cdot\mathbf{q}\,\mathrm{d}V\mathrm{d}t \;=\; \text{constant}. \tag{10}$$

The above relation is an elaboration of the generalized Green's identity. The adjoint boundary / initial conditions are defined such that the constant on the RHS is zero. By integration by parts, we find the general result that $-\mathrm{A}\partial/\partial t = \mathrm{A}^+\partial^+/\partial t$. Setting $\mathrm{A}^+ = \mathrm{A}^*$, then $-\partial/\partial t = \partial^+/\partial t$: the adjoint operator evolves backwards in the physical time.

When we follow the DA approach, the adjoint matrix, L_{ij}, is defined through the Euclidean product (in Einstein's notation)

$$q_i^{+*} L_{ij} q_j - q_i L_{ij}^{+*} q_j^{+*} = 0. \tag{11}$$

The above terms are scalars, so the transposition does not change the equation. Hence, we take the transpose of the second term and equate it to the first term:

$$q_i^{+*} L_{ij} q_j = (q_i L_{ij}^{+*} q_j^{+*})^T = q_i^{+*} L_{ji}^{+*} q_j, \implies \qquad L_{ij}^+ = L_{ji}^*. \tag{12}$$

The adjoint matrix is the conjugate-transpose of the direct matrix.

In Magri and Juniper [5] a comparison between the numerical truncation errors between the CA and DA methods is illustrated. For the thermo-acoustic systems considered in this paper, the DA method is more accurate and easier to implement. We show the CA method for the first thermo-acoustic system, an electrically heated Rijke tube, while we use only the DA method for the second thermo-acoustic system, a ducted diffusion flame.

In stability/receptivity analysis, we consider the eigenproblem of (8), which reads

$$\sigma\mathrm{A}\hat{\mathbf{q}} - \mathrm{L}\hat{\mathbf{q}} = 0, \qquad \sigma^+\mathrm{A}^+\hat{\mathbf{q}}^+ - \mathrm{L}^+\hat{\mathbf{q}}^+ = 0. \tag{13}$$

[1] It is necessary and sufficient to have whatever bilinear nondegenerated form. So, the definition of an inner product is a sufficient condition to calculate the adjoint system.

A very important property of the adjoint and direct eigenpairs $\{\sigma_i, \hat{\mathbf{q}}_i\}$, $\{\sigma_j^+, \hat{\mathbf{q}}_j^+\}$ is the bi-orthogonality condition[2] [16]:

$$\left(\sigma_i - \sigma_j^{+*}\right)\left\langle \hat{\mathbf{q}}_j^+, \mathrm{A}\hat{\mathbf{q}}_i \right\rangle = 0, \tag{14}$$

which states that the inner product $\langle \hat{\mathbf{q}}^+, \mathrm{A}\hat{\mathbf{q}} \rangle$ is zero for every pair of eigenfunctions except when $i = j$, as long as $\sigma_j^+ = \sigma_j^*$.

We study the change of the thermo-acoustic stability as a consequence of a generic perturbation of the problem. The aim is to find a formula for the eigenvalue drift caused by a perturbation to the operator. The direct operator is perturbed as $\mathrm{L} + \epsilon\delta\mathrm{L}$, assuming that accordingly: $\sigma_j + \epsilon\delta\sigma_j$, $\hat{\mathbf{q}}_j + \epsilon\delta\hat{\mathbf{q}}_j$, and $\hat{\mathbf{q}}_j^+ + \epsilon\delta\hat{\mathbf{q}}_j^+$. We substitute these into the eigenproblem of (9) and retain terms up to the first order:

$$\begin{aligned}\sigma_j\langle \hat{\mathbf{q}}_j^+, \mathrm{A}\hat{\mathbf{q}}_j\rangle + \epsilon\delta\sigma_j\langle \hat{\mathbf{q}}_j^+, \mathrm{A}\hat{\mathbf{q}}_j\rangle + \sigma_j\langle \epsilon\delta\hat{\mathbf{q}}_j^+, \mathrm{A}\hat{\mathbf{q}}_j\rangle + \sigma_j\langle \hat{\mathbf{q}}_j^+, \mathrm{A}\epsilon\delta\hat{\mathbf{q}}_j\rangle = \dots \\ \dots = \langle \hat{\mathbf{q}}_j^+, \mathrm{L}\hat{\mathbf{q}}_j\rangle + \langle \epsilon\delta\hat{\mathbf{q}}_j^+, \mathrm{L}\hat{\mathbf{q}}_j\rangle + \langle \hat{\mathbf{q}}_j^+, \epsilon\delta\mathrm{L}\hat{\mathbf{q}}_j\rangle + \langle \hat{\mathbf{q}}_j^+, \mathrm{L}\epsilon\delta\hat{\mathbf{q}}_j\rangle.\end{aligned} \tag{15}$$

We know that $\sigma_j\langle \hat{\mathbf{q}}_j^+, \mathrm{A}\hat{\mathbf{q}}_j\rangle = \langle \hat{\mathbf{q}}_j^+, \mathrm{L}\hat{\mathbf{q}}_j\rangle$ and so $\sigma_j\langle \delta\hat{\mathbf{q}}_j^+, \mathrm{A}\hat{\mathbf{q}}_j\rangle = \langle \delta\hat{\mathbf{q}}_j^+, \mathrm{L}\hat{\mathbf{q}}_j\rangle$. Interestingly, $\sigma_j\langle \hat{\mathbf{q}}_j^+, \mathrm{A}\delta\hat{\mathbf{q}}_j\rangle = \langle \hat{\mathbf{q}}_j^+, \mathrm{L}\delta\hat{\mathbf{q}}_j\rangle$ because taking the inner products of $\delta\hat{\mathbf{q}}_j$ and $\mathrm{L}\delta\hat{\mathbf{q}}_j$ with $\hat{\mathbf{q}}_j^+$ extracts only the components that are parallel to $\hat{\mathbf{q}}_j$ (see eqn. (14)), for which $\mathrm{L}\hat{\mathbf{q}}_j = \sigma_j\mathrm{A}\hat{\mathbf{q}}_j$. This means that the eigenvalue drift is, at first order, as follows

$$\delta\sigma_j = \frac{\langle \hat{\mathbf{q}}_j^+, \delta\mathrm{L}\hat{\mathbf{q}}_j\rangle}{\langle \hat{\mathbf{q}}_j^+, \mathrm{A}\hat{\mathbf{q}}_j\rangle}. \tag{16}$$

Note that the denominator is always different from zero. This is because the dimension of the adjoint space is equal to the original space's dimension, under not restrictive conditions. Choosing a precise eigenpair $\{\sigma, \hat{\mathbf{q}}\}$, the DA approach gives similarly

$$\delta\sigma = \frac{\hat{q}_i^{+*}\delta L_{ij}\hat{q}_j}{\hat{q}_l^{+*}\mathrm{A}_{lk}\hat{q}_k}. \tag{17}$$

Both eqn. (16) and (17) show that, once the perturbation operator/matrix is known, we can evaluate exactly at first order the eigenvalue drift. To this end, we need to solve for two eigenproblems to obtain the dominant direct and adjoint eigenfunctions, $\hat{\mathbf{q}}$ and $\hat{\mathbf{q}}^+$, respectively. This greatly reduces the number of computations without affecting the accuracy.

4.2 What does the adjoint function represent?

In this section we show that the adjoint field quantifies the system's receptivity to open-loop forcing. Then, we will give an interpretation of the adjoint eigenfunctions for the thermo-acoustic systems under investigation. In flow instability, the adjoint equations are interpreted and described by many authors, among which [3, 16, 17, 18, 19, 20, 21, 22]. In this paper, we extend these methods to thermo-acoustic instability. We consider the direct inhomogeneous linear problem (8), with harmonic forcing at complex frequency, σ_s. The initial condition at $t = 0$ is denoted $\mathbf{q}_0$. The general solution of this problem is: $\mathbf{q} = \hat{\mathbf{q}}_s \exp(\sigma_s t) + \mathbf{q}_d + \mathbf{q}_{cs}$, where $\hat{\mathbf{q}}_s \exp(\sigma_s t)$ is the particular solution, $\mathbf{q}_d = \sum_j \beta_j \hat{\mathbf{q}}_j \exp(\sigma_j t)$ is the discrete-eigenmodes solution, and $\mathbf{q}_{cs}$ is the continuous-spectrum solution. We assume that the continuous-spectrum is zero because our domain is bounded. Taking advantage of the bi-orthogonality condition (14), the amplitude of the solution of the linear system, $\mathbf{q}$, can be expressed as:

$$\mathbf{q} = \sum_{j=1}^{N} \left\langle \hat{\mathbf{q}}_j^+, \hat{\mathbf{q}}_0 \exp(\sigma_j t) + \hat{\mathbf{s}}\frac{\exp(\sigma_s t) - \exp(\sigma_j t)}{\sigma_s - \sigma_j} \right\rangle \frac{\hat{\mathbf{q}}_j}{\left\langle \hat{\mathbf{q}}_j^+, \mathrm{A}\hat{\mathbf{q}}_j \right\rangle}. \tag{18}$$

[2] This follows the definition of adjoint space.

The response of the j^{th} eigenfunction component of $\mathbf{q}$ increases as (i) the forcing frequency, σ_s approaches the j^{th} eigenvalue, σ_j; ii) the spatial structure of the forcing, $\hat{\mathbf{s}}$, approaches the spatial structure of the adjoint mode, $\hat{\mathbf{q}}_j^+$; iii) the spatial structure of the initial condition, $\hat{\mathbf{q}}_0$, approaches the spatial structure of the adjoint mode, $\hat{\mathbf{q}}_j^+$. This shows that the sensitivity of the response (called *receptivity*) of each eigenfunction to changes in the spatial structure of the forcing is quantified by the adjoint eigenfunction, $\hat{\mathbf{q}}_j^+$. Hence, the adjoint functions can be regarded as Lagrange multipliers from a constrained optimization perspective [23]. Therefore, u^+ is the Lagrange multiplier of the acoustic momentum equation, revealing the locations where the system is most receptive to a given force; p^+ is the Lagrange multiplier of the energy equation revealing the locations where the system is most receptive to a given heat injection; z^+ is the Lagrange multiplier of the flame equation, revealing in which regions the flame is most receptive to species injection.

5 Results

5.1 Structural sensitivity of the electrically heated Rijke tube

We define a passive device to be an object that causes feedback between the state variables and the governing equations at the position where it is placed. In the language of active control, the sensor and actuator are co-located and there is a fixed relationship between the observation (which is derived from the state variables at that point) and the actuation (the forcing terms in the governing equations).

The continuous adjoint equations of the electrically heated Rijke tube (1)-(2) are:

$$\rho\frac{\partial u^+}{\partial t}+\frac{\partial p^+}{\partial x}+\frac{\sqrt{3}}{2}\beta\left(p_f^+ +\tau\left(\frac{\partial p^+}{\partial t}\right)_f\right)\delta_f=0, \qquad \frac{\partial u^+}{\partial x}+\frac{\partial p^+}{\partial t}-\zeta p^+=0. \tag{19}$$

In this section, the direct and adjoint eigenfunctions are computed by considering a hot wire as a heat source. The parameters are such that the first acoustic mode is the most unstable but the analysis can be repeated for the cases when second or higher modes are most unstable [5, 6]. The direct and conjugate adjoint eigenfunctions are arranged as column vectors $[\hat{u}\ \hat{p}]^T$ and $[\hat{u}^{+*}\ \hat{p}^{+*}]^T$, respectively. The structural sensitivity tensor is defined as follows:

$$S\equiv\frac{\delta\sigma}{\delta\mathbf{C}}=\frac{[\hat{u}^{+*}\ \hat{p}^{+*}]^T\otimes[\hat{u}\ \hat{p}]^T}{\int_0^1(\hat{u}\hat{u}^{+*}+\hat{p}\hat{p}^{+*})\mathrm{d}x+\frac{\sqrt{3}}{2}\beta\tau\hat{u}_f\hat{p}_f^{+*}}. \tag{20}$$

Each component of this structural perturbation tensor quantifies the effect of a feedback mechanism between the j^{th} eigenfunction and the i^{th} governing equation. Therefore we can identify the device that is most effective at changing the frequency or growth rate of the system. The four components of S are shown in fig. 1 as a function of x, which is the location where the passive device (structural perturbation) sits, both when $T_2/T_1=1$ (no temperature jump) or $T_2/T_1=1.6$ (typical temperature jump in the Rijke tube). First, we consider a force in the momentum equation that is proportional to the velocity at a given point ($S_{11}\sim\hat{u}\hat{u}^{+*}$). For example, this could be the (linearized) drag force about an obstacle in the flow. This type of feedback greatly affects the growth rate but hardly affects the frequency, in agreement with Dowling [14]. The real part of S_{11} is positive for all values of x, which means that, whatever value of x is chosen, the growth rate will decrease if the forcing is in the opposite direction to the velocity. This tells us that the drag force about an obstacle in the flow will always stabilize the thermo-acoustic oscillations but is most effective if placed at the upstream or downstream end of this duct. Considering the temperature jump suggests that the most effective place is at the downstream of the duct. Furthermore, by inspection of the amplitudes of the black lines in fig. 1, we see that this is the most effective passive device. Secondly, we consider a feedback mechanism that is proportional to the pressure and that forces the pressure equation ($S_{22}=\hat{p}\hat{p}^{+*}$). The pressure-coupled heat release, which arises in solid rocket engines, is an example of this type of feedback. For this feedback, the system is most sensitive around the centre of the duct. As for S_{11}, this feedback greatly affects the growth rate but hardly affects the frequency, and is positive for all values of x. If the heat release increases with the

pressure, as it does for most chemical reactions, this feedback mechanism is destabilizing. But if a fuel with the opposite behaviour could be found then it would most stabilize the oscillations if placed at the centre of the duct. Thirdly, we consider feedback from the pressure into the momentum equation ($S_{12} = \hat{p}\hat{u}^{+*}$) and feedback from the velocity into the pressure equation ($S_{21} = \hat{u}\hat{p}^{+*}$) . These types of feedback hardly affect the growth rate but greatly affect the frequency. A control hot wire with $\tau \approx 0$ causes this type of feedback (S_{21}), so this analysis shows that it will be relatively ineffective at stabilizing thermo-acoustic oscillations. We illustrate the structural sensitivity to a second hot wire, denoted

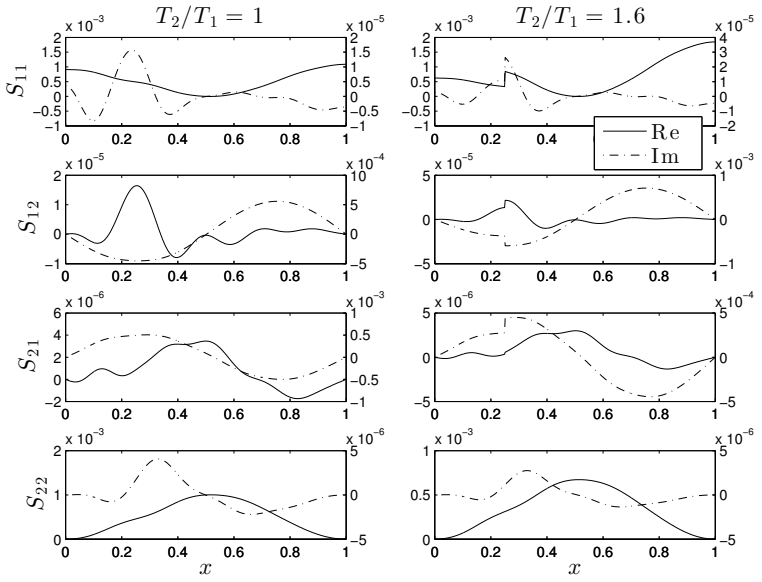

Figure 1: Components of the structural sensitivity tensor. Each component quantifies the effects of a feedback mechanism, placed at x, on the linear growth rate (solid line/left scale) and angular frequency (dashed line/right scale) of the oscillations. Solutions with no temperature jump (left frames) and with temperature jump (right frames). $c_1 = 0.01$, $c_2 = 0.001$, $\tau = 0.01$, $\beta = 0.39$, $x_f = 0.25$.

with the subscript c in fig. 2. We compare the structural sensitivity results with those calculated using the Rayleigh Index. The feedback from the control wire is proportional to the velocity perturbation and perturbs the pressure equation. The structural perturbation tensor therefore has only one component: $\delta C_{21} = \delta\beta_c(1-\sigma\tau_c)$. It has long been known that if pressure and heat-release fluctuations are in phase, then acoustic vibrations are encouraged. More precisely, the Rayleigh criterion states that the energy of the acoustic field grows over one cycle of oscillation if $\oint_T \int_{\mathscr{D}} p\dot{q}\,\mathrm{d}\mathscr{D}\mathrm{d}t$, exceeds the damping, where $\mathscr{D}$ is the flow domain and T is the period. It is particularly informative to plot the spatial distribution of $\oint_T p\dot{q}\,\mathrm{d}t$ which is known as the Rayleigh Index. This reveals the regions of the flow that contribute most to the Rayleigh Criterion and therefore gives insight into the physical mechanisms that alter the amplitude of the oscillation. To examine the effect of the control wire, we substitute the approximate expressions $p = \hat{p}\exp(\sigma_i t)$ and $\dot{q} = \hat{\dot{q}}\exp(\sigma_i t)$ into the Rayleigh index and integrate over a period $2\pi/\sigma_i$, where $\sigma_i = \mathrm{Im}(\sigma)$. (The approximation arises because the growth rate over the cycle has been ignored.) The real part of the Rayleigh Index gives the change in the growth rate and the imaginary part gives the change in the frequency (bottom frames in fig. 2). As expected, the sign of the Rayleigh index matches that of the structural sensitivity (top frames in fig. 2) and the shape is similar.

For smooth variations of the cross-sectional area, the non-dimensional energy equation (1)-(2) can be rewritten [6] as

$$\frac{\partial p}{\partial t} + \frac{\partial u}{\partial x} + \zeta p - \frac{\sqrt{3}}{2}\beta\left(u_f - \tau\left(\frac{\partial u}{\partial t}\right)_f\right)\delta_f = -u_c\frac{1}{\gamma}\frac{\partial \gamma}{\partial x}\theta_c \tag{21}$$

with $\gamma \equiv A(x)/A_0$, where $A(x)$ is the area at location x and A_0 is the area at the mouth of duct. θ_c is 1 at

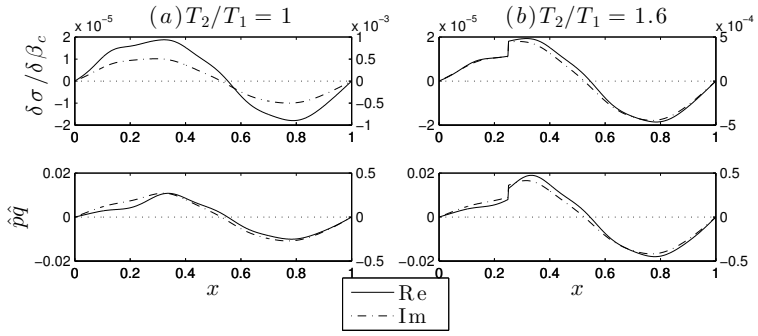

Figure 2: Top frames: structural sensitivity of the growth rate, Re($\delta\sigma/\delta\beta_c$), and of the angular frequency, Im($\delta\sigma/\delta\beta_c$),when a hot wire is placed at location x_c. Bottom frames: Rayleigh index for a control hot wire places at x_c. Solutions with no temperature jump (left frames) and with temperature jump (right frames). Parameters as in fig. 1.

$x = x_c$ and zero elsewhere. A " local smooth cross-sectional area variation", defined such that $\partial\gamma/\partial x\theta_c$ is finite, can be regarded as another passive feedback mechanism. We assume that the area of the duct is constant except at location $x = x_c$, where there is a small smooth change in the area. If γ varies, the RHS of eqn. (21) shows that a change in the area can be interpreted as a forcing term, proportional to $-u_c$, acting on the energy equation. The structural sensitivity is provided by the negative of S_{21} in eqn. (20). Therefore the eigenvalue drift caused by this feedback mechanism is $\delta\sigma = -(\partial\gamma/\partial x)S_{21}(1/\gamma)$. This means that where a control hot wire has a stabilizing effect, a positive change in area in the same location has a destabilizing effect, and vice versa. The inclusion of the temperature jump in the calculation of such sensitivities sharpens the discontinuity of the eigenfunctions at the heat-source location. The shapes and values, however, do not change considerably.

6 Base-state sensitivity and receptivity to species injection of ducted diffusion flames

The structural sensitivity gives the effect of adding a passive feedback device to the system. The base-state sensitivity gives the effect of altering the thermo-acoustic system without adding any passive devices. The base-state sensitivity is calculated directly from the discretized governing equations (the DA method). There are four stages in this method: (1) calculate the perturbation matrix $\delta\mathbf{L}$, imposing a sufficiently small perturbation on the base-state parameter; (2) calculate the eigenvectors of the direct matrix, $\mathbf{L}$, and adjoint matrix, $\mathbf{L}^{*T}$; (3) apply formula (17) to find the eigenvalue drift; (4) divide the eigenvalue drift by the small perturbation used to produce $\delta\mathbf{L}$ at step 1. In this section, the base-state sensitivity analysis is used to calculate how the flame shape affects the growth rate and frequency of the thermo-acoustic oscillations. This is a particularly interesting application because combustion technologists have some control over the flame shape. In this model, the flame shape is determined by the Péclet number, Pe, the stoichiometric mixture fraction, Z_{sto}, and the duct half width, α. $1/\beta_T = (T_i + T_{ad})/2$ is the mean temperature of the flame (β is denoted β_T in this section), where T_i is the inlet (initial) temperature and T_{ad} is the adiabatic temperature. Here, the heat-release parameter is fixed at $\beta_T = 0.67/2$ and the flame position at $x_f = 0.25$, at which point this thermo-acoustic system is marginally stable when $Pe = 35$, $Z_{sto} = 0.8$ and $\alpha = 0.35$. Maps of the base-state sensitivity are shown in figs. 3-4. These correspond to overventilated (i.e. closed) flames because $Z_{sto} > \alpha$. Fig. 3 shows the sensitivity coefficients $\delta\sigma/\delta Z_{sto}$ and $\delta\sigma/\delta\alpha$ as a function of α and Z_{sto}. Fig. 4 shows the sensitivity coefficients $\delta\sigma/\delta Pe$ and $\delta\sigma/\delta\beta_T$ as a function of Pe and β_T. Left frames of figs. 3-4, show the rate of change of growth rate and right frames show the change of the angular frequency. Global information of these maps is summarized in numbers in table 1 as mean values plus standard deviations in %, in the first row, and maximum and minimum values in % in the second and third row, respectively. These maps, obtained

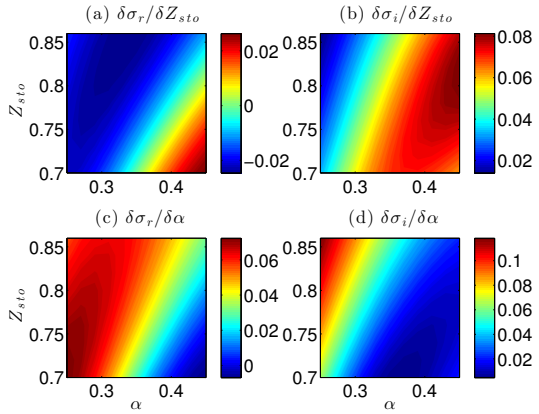

Figure 3: Base state sensitivity of a ducted diffusion flame (I).

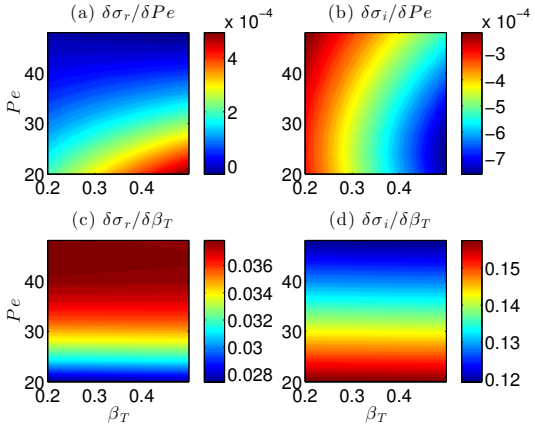

Figure 4: Base state sensitivity of a ducted diffusion flame (II).

$\frac{\delta\sigma_r}{\delta Z_{sto}}$	$\frac{\delta\sigma_i}{\delta Z_{sto}}$	$\frac{\delta\sigma_r}{\delta\alpha}$	$\frac{\delta\sigma_i}{\delta\alpha}$
$-1.097\times10^{-2}\pm46.5\%$	$5.554\times10^{-2}\pm3.7\%$	$4.44\times10^{-2}\pm11.6\%$	$4.405\times10^{-2}\pm17\%$
max = 244	max=148%	max=165%	max=295%
min = −224%	min=25.2%	min=-15.6%	min=11.7%
$\frac{\delta\sigma_r}{\delta Pe}$	$\frac{\delta\sigma_i}{\delta Pe}$	$\frac{\delta\sigma_r}{\delta\beta_T}$	$\frac{\delta\sigma_i}{\delta\beta_T}$
$1.35\times10^{-4}\pm30\%$	$-4.73\times10^{-4}\pm3.8\%$	$3.48\times10^{-2}\pm0.17\%$	$13.8\times10^{-2}\pm0.01\%$
max = 368	max=-45.3%	max=109%	max=115%
min = −23%	min=-161%	min=79%	min=87%

Table 1: Summary of the spatial sensitivities calculated via adjoints in figs. 3-4. σ_r and σ_i are the real and imaginary parts of the eigenvalue. These are the growth rate and angular frequency of the linear system, respectively.

via adjoints, have been checked against the exact solutions obtained (expensively) via finite difference and agree to a tolerance of 10^{-9}. Further details on the parameters used and the numerical treatment will be available in Magri and Juniper [12].

Fig. 3 and table 1 show that the stability of the system is much more sensitive to the stoichiometric mixture fraction, Z_{sto}, the fuel width, α, the heat release parameter, β_T than to the Péclet number, Pe. Figs. 3-4 show that, around these operating points:

- at a given α, small increases of δZ_{sto}, which tend to shorten the flame, make the system more stable when the unperturbed flame is sufficiently short (cold colours, fig. 3a) but make the system more unstable when the unperturbed flame is sufficiently long (hot colours, fig. 3a). Whatever the flame length, small increases δZ_{sto} tend to increase the oscillation frequency (fig. 3b);
- at a given Z_{sto}, small increases of $\delta\alpha$, which tend to lengthen the flame, make the system more unstable especially when the unperturbed flame is short (hot colours, fig. 3c) and increase the angular frequency in any case (fig. 3d);
- the thermo-acoustic system is less sensitive to changes of δPe (fig. 4a). A positive perturbation δPe, which lengthens the flame, tends to decrease the oscillation frequency in any case (fig. 4b);
- little changes of the heat-release parameter $\delta\beta_T$, inversely proportional to the average flame temperature, has always a stabilizing action (fig. 4c) and increase the frequency markedly (fig. 4d). The

sensitivity of the growth rate to $\delta\beta_T$ is higher when the flame is longer (hot colours (fig. 4c). Contrariwise, the sensitivity of the frequency to $\delta\beta_T$ is higher when the flame is shorter (cold colours (fig. 4d).

Therefore, this base-state sensitivity analysis allows a combustion technologist to quickly examine the stability of a given model, and how the stability varies with the parameters of the model, over a wide range of parameter space. On a cautionary note, the results are of course only as good as the model from which they are derived.

In fig. 5 the marginally stable direct eigenfunction, $\hat{z}$, is depicted in frames a,b,c. The corresponding adjoint eigenfunction is depicted in frames d,e,f. The direct eigenfunction is the shape of the oscillation in the long time limit. The adjoint eigenfunction shows the regions of the flame which are most receptive to species injection. This means that we can control the frequency of the flame oscillation, and so the acoustic instability, and make the amplitude of the oscillation decay with an open-loop species injection.

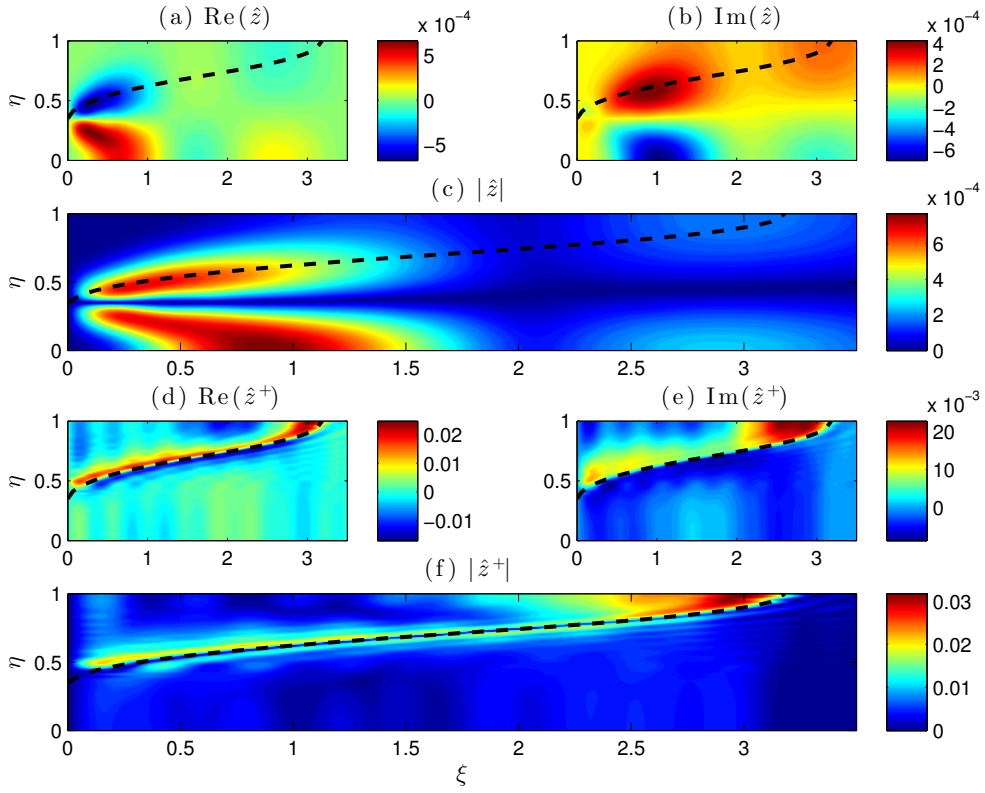

Figure 5: Direct eigenfunction (a-b-c) and corresponding adjoint eigenfunction (d-e-f) of a marginally stable open flame. The areas in which the adjoint eigenfunction is higher are most receptive to species injection as an open-loop control strategy. Parameters: $Z_{sto} = 0.135$, $\alpha = 0.35$, $\beta_T = 1.316/2$, $x_f = 0.25$.

7 Conclusions

The aim of this paper is to introduce adjoint sensitivity analysis to thermo-acoustic systems. We consider a Rijke tube containing an electrically heated wire and a duct containing a diffusion flame. By combining information from the direct and adjoint equations, we predict how the least stable / most unstable eigenvalue of these thermo-acoustic systems changes when a generic passive feedback device

is introduced. From this we find that devices that exert a drag force on the fluid have the biggest effect on the growth rate. Two physical feedback mechanisms in particular are investigated: a second heat source placed in another location along the duct (a second hot wire), and a local smooth variation of the tube cross-sectional area. We find that these feedback mechanisms have more effect on the frequency of oscillations than on their growth rate. Including the temperature jump induced by the compact heat source has not altered qualitatively the results obtained.

In the base-state sensitivity analysis we investigate how tiny variations in the base-state parameters affect the most unstable eigenvalue of the system. This reveals how best to change these parameters in order to stabilize the system and also which base-state parameters have most influence on the stability. For the marginally stable ducted diffusion flame, we find that the system is only slightly sensitive to small perturbations of the Péclet number whereas the growth rate is sensitive to small changes of δZ_{sto}, $\delta\beta_T$, $\delta\alpha$, all of which strongly affect the shape of the flame. This suggests that the role of the flame length is important because it governs the delay between velocity and heat-release oscillation. Future investigations will quantitatively bring to light the role of the flame length in thermo-acoustic instabilities of diffusion flames. Finally, the receptivity maps of a marginally stable flame are calculated for locating the most sensitive regions to injection of species as an open-loop control strategy.

The sensitivity analysis proposed in this paper has been carried out by linearizing the nonlinear governing equations around fixed points. Therefore, we have studied how to extend the linear stable region of fixed points by changing some parameters of the system or introducing passive devices. In future work, we will apply adjoint Floquet analysis to study the stability and control of nonlinear self-sustained oscillations by linearizing the equations around these periodic solutions. We will also examine more realistic acoustic networks with a state-space implementation of an acoustic network model.

The authors would like to thank Prof. Sujith and Dr. Balasubramanian for their valuable discussions on the Galerkin method. L.M. is grateful to Paola Stefanello and Anna Mariani for their proofreading. L.M. is supported by the European Research Council through Project ALORS 2590620. This financial support is gratefully acknowledged.

References

[1] T. C. Lieuwen and V. Yang. *Combustion Instabilities in Gas Turbine Engines: Operational Experience, Fundamental Mechanisms, and Modeling*. American Institute of Aeronautics and Astronautics, Inc., 2005.

[2] D. C. Hill. A theoretical approach for analyzing the restabilization of wakes. *NASA Technical memorandum 103858*, 1992.

[3] F. Giannetti and P. Luchini. Structural sensitivity of the first instability of the cylinder wake. *Journal of Fluid Mechanics*, 581:167–197, 2007.

[4] O. Marquet, D. Sipp, and L. Jacquin. Sensitivity analysis and passive control of cylinder flow. *Journal of Fluid Mechanics*, 615:221–252, November 2008.

[5] L. Magri and M. P. Juniper. Sensitivity analysis of a time-delayed thermo-acoustic system via an adjoint-based approach. *Journal of Fluid Mechanics*, 719:183–202, 2013.

[6] L. Magri and M. P. Juniper. A novel theoretical approach to passive control of thermo-acoustic oscillations: application to ducted heat sources. In *Proceedings of ASME Turbo Expo GT2013-94344*, 2013.

[7] K. Matveev. *Thermoacoustic Instabilities in the Rijke Tube: Experiments and Modeling*. PhD thesis, Caltech Institute of Technology, 2003.

[8] K. Balasubramanian and R. I. Sujith. Thermoacoustic instability in a Rijke tube: Non-normality and nonlinearity. *Physics of Fluids*, 20(4):044103, 2008.

[9] M. P. Juniper. Triggering in the horizontal Rijke tube: non-normality, transient growth and bypass transition. *Journal of Fluid Mechanics*, 667:272–308, November 2010.

[10] M. Tyagi, S. R. Chakravarthy, and R. I. Sujith. Unsteady combustion response of a ducted non-premixed flame and acoustic coupling. *Combustion Theory and Modelling*, 11(2):205–226, April 2007.

[11] K. Balasubramanian and R. I. Sujith. Non-normality and nonlinearity in combustion-acoustic interaction in diffusion flames. *Journal of Fluid Mechanics*, 594:29–57, 2008.

[12] L. Magri and M. P. Juniper. Adjoint sensitivity analysis of ducted diffusion flames for control of thermo-acoustic instabilities. *to be submitted*, 2013.

[13] M. A. Heckl. Non-linear acoustic effects in the Rijke tube. *Acustica*, 72:63–71, 1990.

[14] A. P. Dowling. The calculation of thermoacoustic oscillations. *Journal of sound and vibration*, 180(4):557–581, 1995.

[15] D. Zhao. Transient growth of flow disturbances in triggering a Rijke tube combustion instability. *Combustion and Flame*, 159(6):2126–2137, June 2012.

[16] H. Salwen and C. E. Grosch. The continuous spectrum of the Orr-Sommerfeld equation. Part 2. Eigenfunction expansions. *Journal of Fluid Mechanics*, 104:445–465, April 1981.

[17] D. C. Hill. Adjoint systems and their role in the receptivity problem for boundary layers. *Journal of Fluid Mechanics*, 292:183–204, April 1995.

[18] P. J. Schmid and D. S. Henningson. *Stability and transition of shear flows*. Springer, New York, 2001.

[19] L. Marino and P. Luchini. Adjoint analysis of the flow over a forward-facing step. *Theoretical and Computational Fluid Dynamics*, 23(1):37–54, November 2009.

[20] D. Sipp, O. Marquet, P. Meliga, and A. Barbagallo. Dynamics and Control of Global Instabilities in Open-Flows: A Linearized Approach. *Applied Mechanics Reviews*, 63(3):030801, 2010.

[21] G. J. Chandler. *Sensitivity analysis of low-density jets and flames*. PhD thesis, University of Cambridge, 2010.

[22] G. J. Chandler, M. P. Juniper, J. W. Nichols, and P. J. Schmid. Adjoint algorithms for the Navier–Stokes equations in the Low Mach Number limit. *Journal of Computational Physics*, 231(4):1900–1916, 2011.

[23] M. D. Gunzburger. *Inverse design and optimisation methods. Introduction into mathematical aspects of flow control and optimization*. von Karman Insitute for Fluid Dynamics, Lecture Series 1997-05., 1997.